

Angular correlation function of wave scattering by a random rough surface and discrete scatterers and its application in the detection of a buried object

Guifu Zhang and Leung Tsang

Electromagnetics and Remote Sensing Laboratory, Department of Electrical Engineering,
University of Washington, Box 352500, Seattle, WA 98195-2500, USA

Received 20 January 1997

Abstract. The scattering of waves by a buried object is often obscured by the clutter around it. Such clutter can be attributed to the scattering by random rough surfaces and random discrete scatterers. Recent studies show that, because of the memory effect, the angular correlation function can suppress the effects of clutter and make the scattering by the buried object more conspicuous. In this paper, we study the angular correlation function of wave scattering by a buried object underneath a layer of random discrete scatterers and a non-Gaussian random rough surface. Such problems are common when the target is buried below a rough surface that is underneath a layer of vegetation. Numerical results are illustrated for various parameters of rough surfaces and discrete scatterers. The angular correlation function is calculated by frequency and angular averaging. It is shown that the use of the angular correlation function can enhance target detection in the presence of clutter.

1. Introduction

Wave scattering by random rough surfaces has been studied extensively using analytic techniques [1, 2], laboratory experimental measurements [3], and numerical simulations [4]. Recent numerical simulations have been performed for 1D and 2D rough surfaces and for impenetrable and penetrable rough surfaces [5–7]. Direct applications of the studies have been made for remote sensing of natural surfaces such as soils, snow surfaces and sea surfaces [8]. Most of the studies have utilized the bistatic scattering intensities to characterize the scattering results. Recently, a paper by Feng *et al* demonstrated the existence of memory effects by taking the angular correlation of wave scattering [9]. The angular correlation function is the correlation function of two scattered fields in directions θ_{s2} and θ_{s1} corresponding to two incident waves in directions θ_{i2} and θ_{i1} , respectively (figure 1). A strong correlation, called the angular memory effect, is exhibited for the transmitting fields and the scattered fields [9–12]. The memory line obeys the angular relation of $\sin \theta_{s2} - \sin \theta_{s1} = \sin \theta_{i2} - \sin \theta_{i1}$. It is analogous to a phase matching condition for reflection by a flat boundary. For rough surface scattering, it has been shown that the values of the angular correlation function (ACF) are small except along the memory line of the incident and scattered directions. Random rough surfaces can be statistically translation invariant. Thus, the surfaces exhibit a phase matching condition when ensemble averages of the scattered fields are taken. This has been verified by theoretical models and experiments [13, 14]. For a single random rough surface, the memory effect of the ACF has also been shown

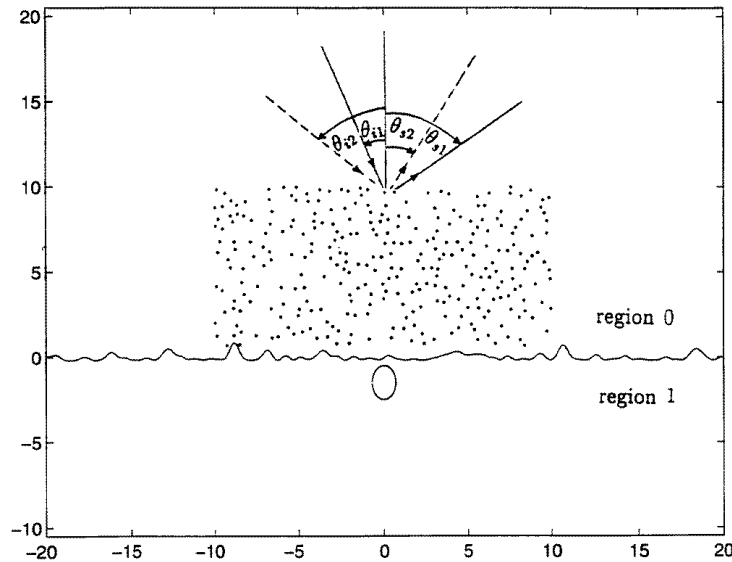


Figure 1. Configuration of wave scattering from a single realization of a non-Gaussian random rough surface with discrete scatterers above and a buried object underneath. This single realization is used in the simulations.

by using frequency averaging [16, 17]. For volume scattering, the same phase matching condition holds for the horizontal direction, $\sin \theta_{i1} - \sin \theta_{s1} = \sin \theta_{i2} - \sin \theta_{s2}$. For the case of a thick layer, an additional phase matching condition is $\cos \theta_{i1} + \cos \theta_{s1} = \cos \theta_{i2} + \cos \theta_{s2}$. The existence of the second condition makes the memory line narrower and shorter.

Recently, the memory effect has been applied to the detection of a buried object [15–17]. When wave scattering techniques are used to detect the presence of a buried object, the scattering of waves by the buried object is often obscured by clutter such as rough surface scattering and random medium scattering. The scattered intensity of clutter can be comparable to or larger than that of the buried object. This makes the detection of a buried object based on scattering intensity difficult. However, by making use of the angular correlation function, one can show that the contribution of clutter to the angular correlation function is minimal away from the memory line, making the contribution of the buried object more conspicuous by many dB.

In this paper, we study the scattering coefficient and angular correlation function of wave scattering by a buried object beneath a layer of random discrete scatterers and a random rough surface (figure 1). This study has applications in the detection of a buried object under a rough soil surface that is below a layer of vegetation. We also use the model of a non-Gaussian rough surface, as it is a closer approximation to a natural surface than a Gaussian rough surface. In the calculation of the angular correlation function, an average is usually taken over realizations. However, this averaging technique is not applicable to detection of a buried object, because the object is buried below a single realization of the rough surface and random discrete scatterers. Thus we calculate the angular correlation function by taking frequency averaging and angular averaging.

In section 2, we formulate the problem by using integral equations that are later solved by the method of moments. In section 3, we define the frequency averaging that is used in calculating the angular correlation function for a single realization of the rough surface

and random discrete scatterers. In section 4, we describe the Weibull random process that is used to generate a non-Gaussian random rough surface. We then calculate the scattering coefficient and the angular correlation function. The memory effect of the non-Gaussian random rough surface is exhibited in both realization and frequency averaging. In section 5, we show the memory effect for volume scattering by frequency averaging. A weight function has to be used to show the memory effect for some cases. In section 6, we show the results for the memory effect when volume scattering and surface scattering are both present, as well as that with a buried object. We also illustrate the application of the angular correlation function in the detection of a buried object in such a complex environment.

2. Formulations

We formulate the problem by using the integral equation method. The equations are solved numerically using the method of moments, giving an exact solution of Maxwell's equations. The discrete random scatterers are above a random rough surface and the buried object is located below the surface as shown in figure 1.

A tapered plane wave $\psi^i(\bar{r})$ is incident on the medium

$$\psi^i(\bar{r}) = \exp[i(kx \sin \theta_i - kz \cos \theta_i)(1 + w(\bar{r}))] \exp[-(x + z \tan \theta_i)^2/g^2] \quad (1)$$

where g is the tapering parameter, and

$$w(\bar{r}) = \frac{2(x + z \tan \theta_i)^2/g^2 - 1}{(kg \cos \theta_i)^2}. \quad (2)$$

For the discrete scatterers, we assume that they are much smaller than one wavelength and we use a volume integral equation. For the rough surface and the buried object, we use surface integral equations. The boundary conditions are $\psi_0 = \psi_1$, $\partial\psi_0/\partial n = \partial\psi_1/\partial n$ at the rough surface and $\psi_1 = 0$ on the surface of the buried object with ψ_0 and ψ_1 being the fields in regions 0 and 1, respectively. The integral equations are as follows:

$$\begin{aligned} - \int_{s_r} \left[\psi(\bar{r}') \frac{\partial G_0(\bar{r}_m, \bar{r}')}{\partial n'} - G_0(\bar{r}_m, \bar{r}') \frac{\partial \psi(\bar{r}')}{\partial n'} \right] ds' + \psi(\bar{r}_m) - \sum_{n=1}^N G_0(\bar{r}_m, \bar{r}_n) A_n \psi(\bar{r}_n) \\ = \psi^i(\bar{r}_m) \end{aligned} \quad (3)$$

$$\begin{aligned} \frac{1}{2} \psi(\bar{r}_r) - \int_{s_r} \left[\psi(\bar{r}') \frac{\partial G_0(\bar{r}_r, \bar{r}')}{\partial n'} - G_0(\bar{r}_r, \bar{r}') \frac{\partial \psi(\bar{r}')}{\partial n'} \right] ds' - \sum_{n=1}^N G_1(\bar{r}_r, \bar{r}_n) A_n \psi(\bar{r}_n) \\ = \psi^i(\bar{r}_r) \end{aligned} \quad (4)$$

$$\frac{1}{2} \psi(\bar{r}_r) + \int_{s_r} \left[\psi(\bar{r}') \frac{\partial G_1(\bar{r}_r, \bar{r}')}{\partial n'} - G_1(\bar{r}_r, \bar{r}') \frac{\partial \psi(\bar{r}')}{\partial n'} \right] ds' + \int_{s_b} G_1(\bar{r}_r, \bar{r}') \frac{\partial \psi(\bar{r}')}{\partial n'} ds' = 0 \quad (5)$$

$$\int_{s_r} \left[\psi(\bar{r}') \frac{\partial G_1(\bar{r}_b, \bar{r}')}{\partial n'} - G_1(\bar{r}_b, \bar{r}') \frac{\partial \psi(\bar{r}')}{\partial n'} \right] ds' + \int_{s_b} G_1(\bar{r}_b, \bar{r}') \frac{\partial \psi(\bar{r}')}{\partial n'} ds' = 0 \quad (6)$$

where s_r is the rough surface, s_b is the surface of the buried object, G_0 and G_1 are the Green's functions in region 0 and region 1, respectively, A_n is the scattering amplitude of the n th scatterer, and \bar{r}_n is the position of the n th discrete scatterer.

Equations (3)–(6) are coupled integral equations. We solve equations (3)–(6) by the method of moments. After the matrix equation is solved, the far-field scattered field in region 0 is calculated by

$$\psi_s(\bar{r}) = \frac{e^{ikr}}{\sqrt{r}} \psi_s^N(\theta_s, \theta_i) \quad (7)$$

and

$$\begin{aligned} \psi_s^N(\theta_s, \theta_i) = & \frac{i}{4} \sqrt{\frac{2}{\pi k}} e^{-i\pi/4} \left\{ \sum_{n=1}^N A_n \psi(\bar{r}_n) \exp(-ik(x_n \sin \theta_s + z_n \cos \theta_s)) \right. \\ & + \int dx' \left[-\sqrt{1 + (f(x'))^2} \frac{\partial \psi(\bar{r}')}{\partial n'} \right. \\ & \left. \left. + \psi(\bar{r}') ik \left(\frac{df}{dx'} \sin \theta_s - \cos \theta_s \right) \right] \exp(-ik(x' \sin \theta_s + f(x') \cos \theta_s)) \right\} \quad (8) \end{aligned}$$

The bistatic scattering coefficient and the angular coerrelation function can be obtained from the normalized scattered field, as given by (8) based on averaging.

3. Averaging techniques

In rough surface and random medium scattering, the average is usually taken by averaging over different samples (realization) with the same statistics. For wave scattering by random rough surfaces or random media, the bistatic scattering coefficient (BSC) is an averaged result of normalized scattering intensities for many realizations of random rough surfaces and random media, as given by

$$\sigma_r(\theta_s, \theta_i) = \frac{1}{N_r} \sum_{n=1}^{N_r} |\psi_s^N(\theta_s, \theta_i; n)|^2 / P \quad (9)$$

where n denotes the realization index, N_r is the number of realizations, and P is the total power flux of the incident wave.

The angular correlation function is the correlation between two scattered fields for two corresponding incident waves. It is written as

$$\Gamma_r(\theta_{s1}, \theta_{i1}; \theta_{s2}, \theta_{i2}) = \frac{1}{N_r} \sum_{n=1}^{N_r} \psi_s^N(\theta_{s1}, \theta_{i1}, n) \psi_s^{N*}(\theta_{s2}, \theta_{i2}, n) / \sqrt{P_1 P_2} \quad (10)$$

where N_r is the number of realizations. P_1 and P_2 are the total power fluxes of the two incident waves. The angular correlation function defined by (10) contains both amplitudes and the phase difference between the two waves. It reduces to (9) as a scattering coefficient.

Realization averaging used in (9) and (10), however, is not applicable to the problem of target detection in which a target is buried below a single realization of a rough surface and a random medium. Frequency averaging is an alternative way of obtaining the averaged result. The angular correlation function is then defined based on frequency averaging as

$$\Gamma_f(\theta_{s1}, \theta_{i1}; \theta_{s2}, \theta_{i2}) = \frac{1}{N_f} \sum_{n=1}^{N_f} W(f_n) \psi_s^N(\theta_{s1}, \theta_{i1}; f_n) \psi_s^{N*}(\theta_{s2}, \theta_{i2}; f_n) / \sqrt{P_1 P_2} \quad (11)$$

where N_f is the number of frequencies over the frequency range $f_0 - \Delta f < f_n < f_0 + \Delta f$, and n is the frequency index for f_n . The weighting function is $W(f_n)$. It is needed when

the frequency averaging is taken over a wide band and the scattering characteristics are strongly frequency dependent.

In frequency averaging, an average is taken by changing wave frequency, which is equivalent to shrinking or enlarging the scattering objects. The samples at different frequencies may not be completely independent. The correlation frequency band depends on the size of the medium [17]. To get enough samples, a wide frequency band is required.

Another alternative way of averaging is angular averaging, which is defined as averaging over small changes of incident and scattering angles around the fixed angles for the angular correlation. It is given by

$$\Gamma_a(\theta_{s1}, \theta_{i1}; \theta_{s2}, \theta_{i2}) = \frac{1}{N_a} \sum_{n=1}^{N_a} \psi_s^N(\theta_{s1} + \delta_n, \theta_{i1} + \delta_n) \psi_s^{N*}(\theta_{s2} + \delta_n, \theta_{i2} + \delta_n) / \sqrt{P_1 P_2} \quad (12)$$

where N_a is the number of angles, and δ_n is the small angular difference for index n . It is usually difficult to obtain many independent samples for a small angular range. However, smooth results can be obtained when frequency averaging is combined with angular averaging.

4. Wave scattering by non-Gaussian rough surfaces

In this section, we illustrate the generation of a non-Gaussian rough surface and the calculation of wave scattering. Both realization averaging and frequency averaging are used to show the memory effect.

4.1. Generation of non-Gaussian rough surfaces

The non-Gaussian random process has been studied and generated by using different approaches [18–20]. A simple way of generating a non-Gaussian random process is to use transformation methods as reviewed by Johnson [21]. Gaussian random rough surfaces can easily be generated by using the spectrum method which has been widely used in the calculation of wave scattering [4]. The Weibull random process can be more flexible and is closer to a natural surface. The Rayleigh and exponential distributions are two degenerate cases of the Weibull distribution. We will obtain Weibull random rough surfaces from Gaussian random rough surfaces using a transformation method. Suppose that Z_1 and Z_2 are two Gaussian random processes with identical distribution given by

$$p(z_1) = p(z_2) = \frac{1}{\sqrt{2\pi}\sigma_G} \exp\left(-\frac{z^2}{2\sigma_G^2}\right). \quad (13)$$

Then, a Weibull random process with a distribution of

$$p(z) = \beta\alpha(\alpha z)^{\beta-1} \exp(-(\alpha z)^\beta) \quad (14)$$

can be constructed as

$$z(x) = (z_1(x)^2 + z_2(x)^2)^{1/\beta} \quad (15)$$

with mean value and variance of

$$\langle Z \rangle = (2\sigma^2)^{1/\beta} \Gamma(1 + 1/\beta) \quad (16)$$

$$\sigma_W^2 = (2\sigma_G^2)^{1/\beta} [\Gamma(1 + 2/\beta) - \Gamma^2(1 + 1/\beta)] \quad (17)$$

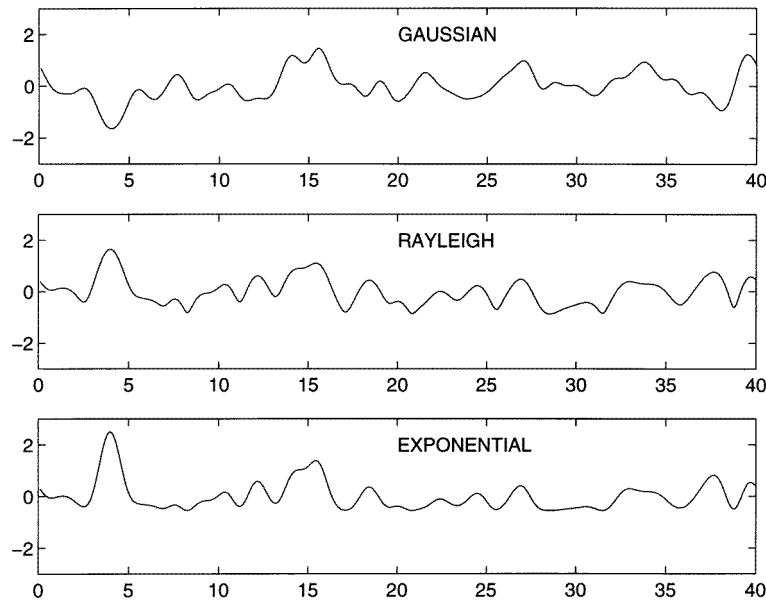


Figure 2. Rough surface profiles for Gaussian (upper), Rayleigh (middle) and exponential (lower) distributions. $h = 0.5\lambda_0$, $l = 1.0\lambda_0$.

where $\Gamma(\cdot)$ is the gamma function. The parameter α of the Weibull distribution is related to σ_G by $\alpha = (2\sigma_G^2)^{-1/\beta}$. The correlation function of the Weibull random process is also related to that of a Gaussian random process:

$$c_W(x) = \left\{ \frac{\Gamma^2(1 + 1/\beta)}{\Gamma(1 + 2/\beta) - \Gamma^2(1 + 1/\beta)} \right\} [F_1(-1/\beta, -1/\beta; c_G^2(x)) - 1] \quad (18)$$

where $F_1(\cdot)$ is the hypergeometric function. When $\beta = 1$, we have $c_W = c_G^2$.

To generate a Weibull random rough surface with given RMS height and correlation function c_W , we only need to find the variance σ_G and the correlation function c_G for the corresponding Gaussian random processes through equations (17) and (18). For simplicity, we use a Gaussian correlation function. For the same RMS height ($h = 0.5\lambda_0$) and correlation length ($l = 1.0\lambda_0$), three random rough surfaces with Gaussian, Rayleigh, and exponential distribution are shown in figure 2. We see that the surface with exponential distribution has fewer but higher bumps than that with Gaussian distribution, and it is not statistically symmetric in the vertical direction.

4.2. Scattering coefficients and angular correlation function of rough surfaces

Figure 3 shows the bistatic scattering coefficients from dielectric rough surfaces with a relative dielectric constant of $\epsilon_r = 3.7 + 0.13i$. The angle of incidence is 30° . All the random rough surfaces have the same RMS height of $h = 0.5\lambda_0$ and correlation length $l = 1.0\lambda_0$. We see that the scattering pattern for Rayleigh rough surfaces is quite close to that for Gaussian rough surfaces. However, the scattering by the exponential rough surfaces is very different from the others. The backscattering coefficient of the exponential rough surfaces is smaller than that of the Gaussian rough surfaces. This is because the RMS height is dominated by the few high bumps, but the mean slope is smaller in the exponential distribution case.

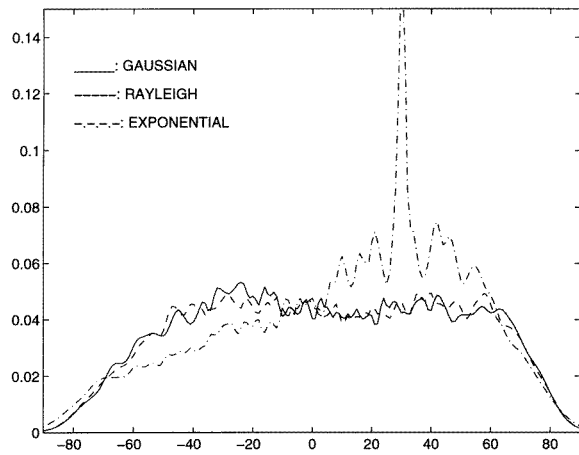


Figure 3. Comparison of bistatic scattering coefficients of the random rough surfaces with Gaussian (—), Rayleigh (---) and exponential (- · -) distributions. Results are obtained by averaging over 100 realizations. $h = 0.5\lambda_0$, $l = 1.0\lambda_0$. The angle of incidence $\theta_1 = 30^\circ$; the dielectric constant of the low medium is $\epsilon_r = 3.7 + 0.13i$.

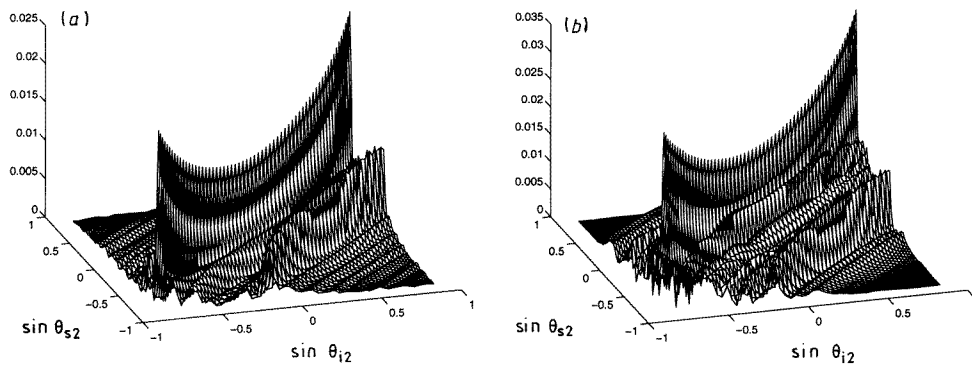


Figure 4. Mesh of angular correlation for wave scattering from rough surface only. The reference angles are $(20^\circ, -20^\circ)$; the dielectric constant of the low medium is $\epsilon_r = 3.7 + 0.13i$. $h = 0.2\lambda_0$, $l = 0.5\lambda_0$, $L = 40\lambda_0$, $g = L/4$. (a) Realization averaging over 100 realizations. (b) Frequency averaging; the averaging band is $0.5f_0 - 1.5f_0$.

Figure 4 shows the 3D plots of the angular correlation function of wave scattering by the exponential rough surfaces with RMS height of $h = 0.2\lambda_0$ and correlation length of $l = 0.5\lambda_0$. We fix a pair of incident and scattering angles of $\theta_{s1} = -20^\circ$ and $\theta_{i1} = 20^\circ$. The other pair of angles of θ_{s2} and θ_{i2} are treated as variables. Figure 4(a) is the result obtained by realization averaging over 100 realizations. The large ridge corresponds to the ψ_2 measured in the forward direction of $\theta_{s2} = \theta_{i2}$. Such ridges can disappear for very rough surfaces [17]. We see a clear line on $\sin \theta_{i2} - \sin \theta_{s2} = 0.684 = \sin \theta_{i1} - \sin \theta_{s1}$. Away from the memory line, the angular correlation function is close to zero. Figure 4(b) shows the result of wave scattering by a single rough surface obtained by frequency averaging. The memory line is also shown. The frequency band is from $0.5f_0$ to $1.5f_0$. Fifty frequencies with the same interval are taken within the band. We note that the frequency-averaged results differ from the realization averaged results.

5. Wave scattering by random discrete scatterers

The volume scattering is simulated by a layer of small cylinders. Both the scattering coefficient and angular correlation function are calculated. 300 cylinders are randomly distributed in the region of $20\lambda_0 \times 10\lambda_0$. The relative dielectric constant is $\epsilon_r = 16.67 + 1.15i$.

Figure 5 shows the bistatic scattering coefficient with an angle of incidence of 20° . The solid and dashed curves are for different cylinders, of radii $a = 0.05\lambda_0$ and $0.015\lambda_0$, respectively. Results are obtained by taking an average over 50 realizations. For $a = 0.015\lambda_0$, it shows almost isotropic scattering, since the scatterers are so small and sparsely distributed, and the first-order scattering is dominant. For $a = 0.05\lambda_0$, the results exhibit backscattering enhancement that is due to multiple scattering.

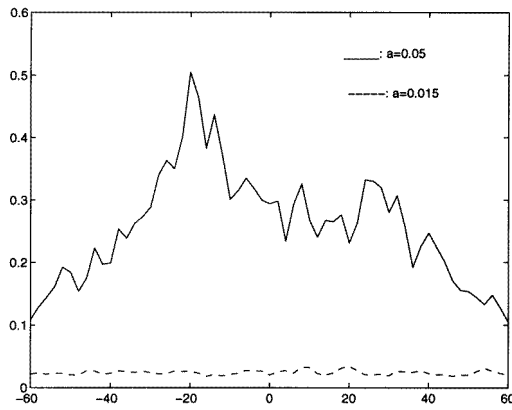


Figure 5. Bistatic scattering coefficients of the random discrete scatterers (50 realizations). The angle of incidence is $\theta_i = 20^\circ$, 300 small cylinders with dielectric constant of $\epsilon_r = 16.67 + 1.15i$. —, $a = 0.05\lambda_0$; ---, $a = 0.015\lambda_0$.

The angular correlation function is shown in figures 6 and 7 for the two cases where the reference angles are $\theta_{s2} = -20^\circ$ and $\theta_{i1} = 20^\circ$. The numerical results shown in figure 6 are for $a = 0.05\lambda_0$. Figure 6(a) is the result of realization averaging over 50 realizations and a clear memory line is shown. The translational invariance in the horizontal direction gives

$$\sin \theta_{i1} - \sin \theta_{i2} = \sin \theta_{s1} - \sin \theta_{s2}. \quad (19)$$

For a thick layer of discrete scatterers, we have an additional condition of translational invariance:

$$-\cos \theta_{i1} + \cos \theta_{i2} = \cos \theta_{s1} - \cos \theta_{s2}. \quad (20)$$

A maximum value can be found for the angles satisfying the above equations, which is called a memory dot. Compared with that of rough surface scattering, the memory line is shorter. For one realization of the discrete scatterers, we use frequency averaging over the frequency band of $0.5f_0$ to $1.5f_0$ to obtain the angular correlation function shown in figure 6(b). The memory line is also shown clearly, but the value of ACF away from the memory line can be large. This is because in frequency averaging we do not have as many independent samples as in realization averaging.

Figure 7 shows the result for $a = 0.015\lambda_0$. The sharp peak is missing in this case, since the first-order scattering is dominant. The result shown in figure 7(a) is obtained by realization averaging and the memory line is shown. The result in figure 7(b) is obtained by frequency averaging without using a weighting function. There are strong fluctuations. Figure 7(c) is the result obtained by the frequency averaging with a weighting function of $(f_0/f)^4$. The result is smoother than figure 7(b) and the memory line is clearly visible.

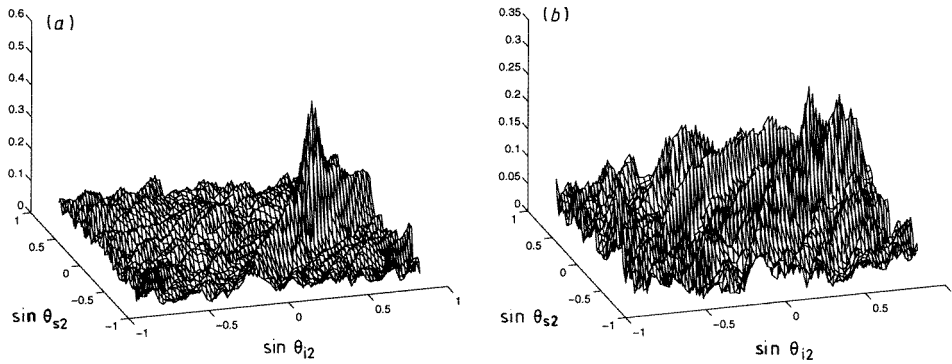


Figure 6. Mesh of angular correlation function for wave scattering by random discrete scatterers. The reference angles are $(-20^\circ, 20^\circ)$; the dielectric constant of the scatterers is $\epsilon_r = 16.67 + 1.15i$. 300 scatterers, each with a radius of $a = 0.05\lambda_0$. (a) Realization averaging over 50 realizations. (b) Frequency averaging with averaging band of $0.5f_0-1.5f_0$.

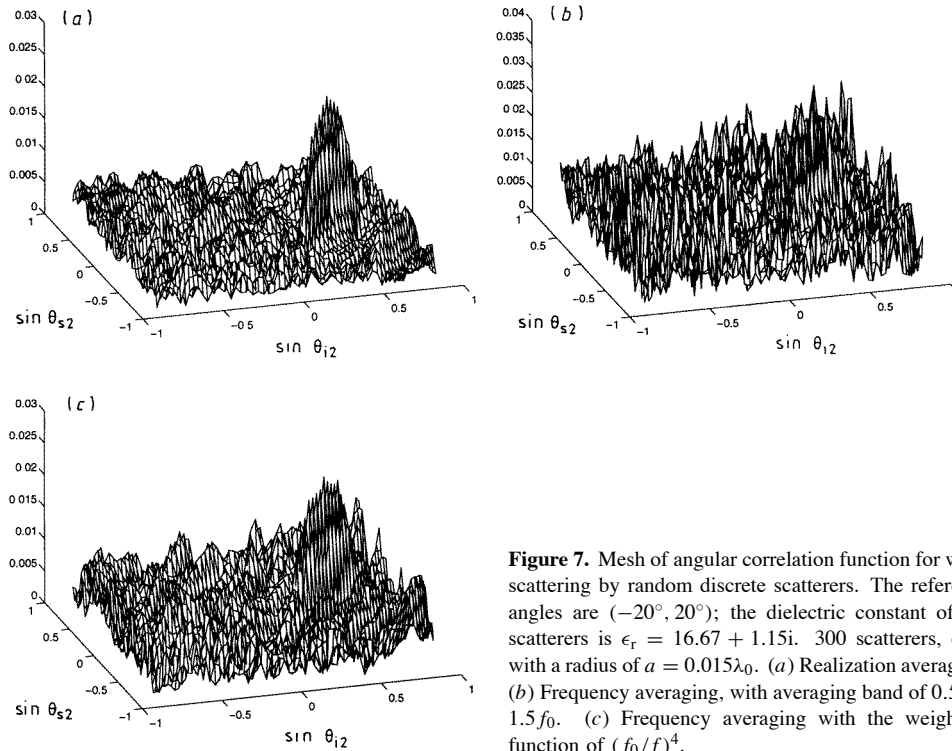


Figure 7. Mesh of angular correlation function for wave scattering by random discrete scatterers. The reference angles are $(-20^\circ, 20^\circ)$; the dielectric constant of the scatterers is $\epsilon_r = 16.67 + 1.15i$. 300 scatterers, each with a radius of $a = 0.015\lambda_0$. (a) Realization averaging. (b) Frequency averaging, with averaging band of $0.5f_0-1.5f_0$. (c) Frequency averaging with the weighting function of $(f_0/f)^4$.

This is because the scattering amplitude for a small scatterer is strongly frequency dependent ($(ka)^2$ for the 2D case). The weighting function, $(f/f_0)^4$, is used so that the samples at each frequency are equally weighted and enough independent samples are obtained.

6. Detection of a buried object in the presence of a rough surface and random discrete scatterers

We have shown results for rough surface scattering and volume scattering. The angular correlation function is now studied for wave scattering by a rough surface co-existing with random scatterers for the detection of a buried object as shown in figure 1. In this case, only one realization of a rough surface and randomly distributed scatterers is involved. Realization averaging is not applicable because the object is buried under a single realization. We use frequency averaging to obtain the angular correlation function. Numerical simulations are performed for an exponential rough surface of $h = 0.2\lambda_0$ and $l = 0.5\lambda_0$ with 300 small scatterers and with or without a buried object. The radius of each small cylinder is $a = 0.01\lambda_0$. The buried object is an elliptical cylinder of $b = 0.7\lambda_0$ in the horizontal direction and $c = 1.0\lambda_0$ in the vertical direction. It is placed at $d = 1.5\lambda_0$ below the mean of the surface. Figure 8(a) is the result without the buried object and figure 8(b) is that with the buried object. Both figures show the memory effect. This means wave scattering by the rough surface and random scatterers is dominant, since wave scattering from a deterministic object does not have the memory effect. The difference in the magnitude of the angular correlation function along the memory line between the results of figure 8(a) and 8(b) is so small that the detection of the buried object is difficult. This means the intensity method does not work well for this case, since the scattered intensity corresponds to a point on the memory line with $\theta_{s2} = \theta_{s1}$ and $\theta_{i2} = \theta_{i1}$. However, we do see the difference away from the memory line.

To further smooth out the fluctuation, we use frequency averaging combined with angular averaging to obtain the angular correlation function and scattering coefficient. The angular correlation function based on combined frequency and angular averaging is given by

$$\Gamma_{fa}(\theta_{s1}, \theta_{i1}; -\theta_{i2}, \theta_{i2}) = \frac{1}{N_a} \sum_{n=1}^{N_a} \Gamma_f(\theta_{s1}, \theta_{i1}; -\theta_{i2} - \delta_n, \theta_{i2} + \delta_n) \quad (21)$$

$$\sigma_{fa}(\theta_s, \theta_i) = \frac{1}{N_a} \sum_{n=1}^{N_a} \sigma_f(\theta_s - \delta_n, \theta_i + \delta_n). \quad (22)$$

To show the effectiveness of the angular correlation method in the detection of a target, we compare the ratio of the angular correlation function with and without a object and that of the bistatic scattering coefficient (BSC). The ratios are defined as follows:

$$\text{ratio of } |\text{ACF}| = \frac{|\text{ACF}| \text{ with buried object}}{|\text{ACF}| \text{ without buried object}} = \frac{|\Gamma_{wb}(\theta_{s1}, \theta_{i1}; \theta_{s2}, \theta_{i2})|}{|\Gamma_{nb}(\theta_{s1}, \theta_{i1}; \theta_{s2}, \theta_{i2})|} \quad (23)$$

$$\text{ratio of BSC} = \frac{\text{BSC with buried object}}{\text{BSC without buried object}} = \frac{\sigma_{wb}(\theta_s, \theta_i)}{\sigma_{nb}(\theta_s, \theta_i)} \quad (24)$$

where wb = ‘with buried object’ and nb = ‘no buried object’. Figure 9 shows the ratios. The solid line is for the ACF and the dashed line for the BSC. The ACF and BSC, as well as their ratios, are evaluated at the backscattering direction with $\theta_{s2} = -\theta_{i2}$. The reference angles are $(\theta_{s1}, \theta_{i1}) = (-20^\circ, 20^\circ)$, $(-60^\circ, 60^\circ)$, as shown in the figure. We can see that the ratio of the ACF is usually larger than the ratio of the BSC. The difference can be as large as 10 dB. It is noted that the large ratio is for the cases when the angle of incidence $\theta_{i2} < 0$. This is because the rough surface is not symmetric, and also the randomness of the phase difference can be large when the angle is large. Thus, for better detection of a target, a wide separation of angular pairs $(\theta_{s1}, \theta_{i1})$ and $(\theta_{s2}, \theta_{i2})$ is desirable.

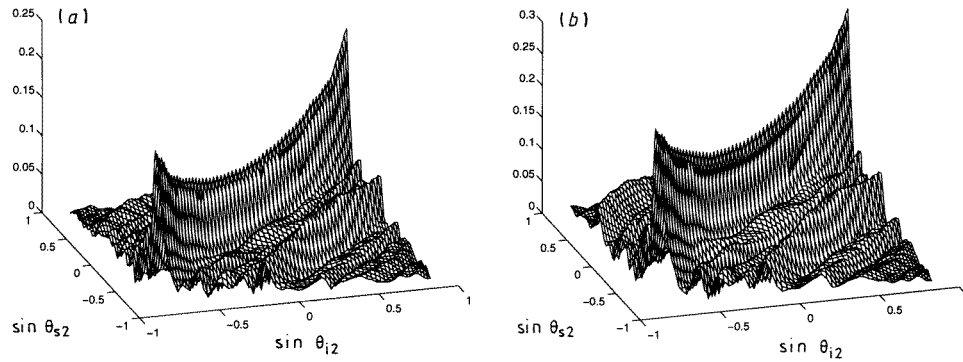


Figure 8. Mesh of angular correlation function by frequency averaging for wave scattering by a rough surface and random discrete scatterers with and without a buried object underneath. Reference angles $(-20^\circ, 20^\circ)$. The rough surface has parameters $h = 0.2\lambda_0$ and $l = 0.5\lambda_0$. The dielectric constant of the low medium is $\epsilon_r = 3.7 + 0.13i$; that of the scatterers is $\epsilon_r = 16.67 + 1.15i$. 300 scatterers, each with a radius of $a = 0.01\lambda_0$. (a) Without buried object. (b) With a buried object of $b = 0.7\lambda_0$ and $c = 1.0\lambda_0$ placed at $d = 1.5\lambda_0$.

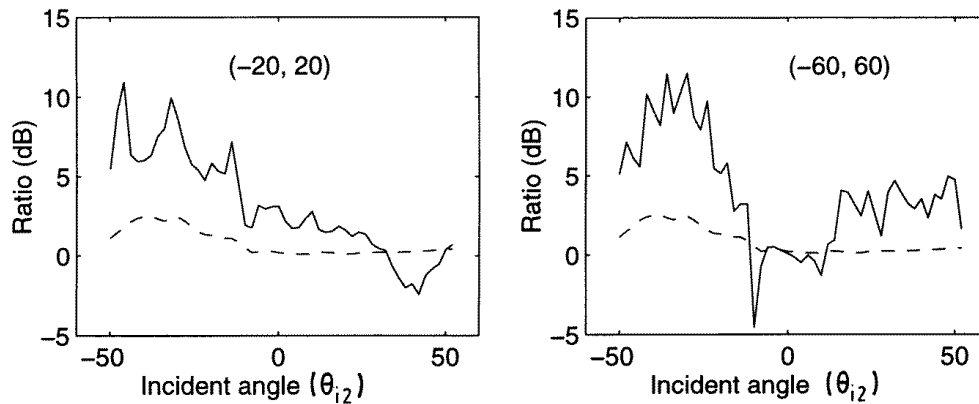


Figure 9. Comparisons between the results for a buried object detection using the angular correlation function and that using the scattering coefficient. $\theta_{s2} = -\theta_{i2}$. —, ratio of the ACF; ---, ratio of the BSC. Left: $(\theta_{s1}, \theta_{i1}) = (-20^\circ, 20^\circ)$. Right: $(\theta_{s1}, \theta_{i1}) = (-60^\circ, 60^\circ)$.

7. Conclusions

We have examined the memory effect for non-Gaussian random rough surfaces and random discrete scatterers. The memory effect of the ACF is shown to have application in target detection, and the signal from the buried object is enhanced with respect to the clutter. In this paper, we have done extensive simulations based on the 2D scattering problem. Presently, we are extending the study to 3D simulations and comparison with real-life radar data.

Acknowledgment

This work has been supported by Office of Naval Research (Grant Number N00014-96-1-0813).

References

- [1] Tsang L, Kong J A and Shin R T 1985 *Theory of Microwave Remote Sensing* (New York: Wiley Interscience)
- [2] Ishimaru A and Chen J S 1991 Scattering from very rough metallic and dielectric surfaces: a theory based on the modified Kirchhoff approximation *Waves Random Media* **1** 21–34
- [3] Phu P, Ishimaru A and Kuga Y 1994 Copolarized and cross polarized enhanced backscattering from manufactured two-dimensional very rough surfaces at millimeter wave frequency *Radio Sci.* **29** 1275–91
- [4] Thorsos E and Jackson D 1991 Studies of scattering theory using numerical methods *Waves Random Media* **1** 165–90
- [5] Tsang L, Chan C H, Pak K and Sangani H 1995 Monte Carlo simulations of large-scale problems of random rough surface scattering and applications to grazing incidence with the BMIA/Canonical grid method *IEEE Trans. Antennas Propagat.* **43** 851–9
- [6] Pak K, Tsang L, Chan C and Johnson J 1995 Backscattering enhancement of vector electromagnetic waves from two-dimensional perfectly conducting random rough surface based on Monte Carlo simulations *J. Opt. Soc. Am.* **12** 2491–9
- [7] Pak K, Tsang L and Johnson J 1997 Numerical simulation and backscattering enhancement of scattered waves from two-dimensional dielectric random rough surfaces with sparse-matrix canonical grid method *J. Opt. Soc. Am.* in press
- [8] Tsang L, Pak K, Weeks R, Shi J C and Rott H 1996 Electromagnetic wave scattering from real-life rough-surface profiles and profiles based on an averaged spectrum *Microwave Opt. Technol. Lett.* **12** 258–62
- [9] Feng S, Kane C, Lee P A and Stone A D 1988 Correlations and fluctuations of coherent wave transmission through disordered media *Phys. Rev. Lett.* **61** 834–7
- [10] Michel T R and O'Donnell K A 1992 Angular correlation functions of amplitudes scattered from a one-dimensional, perfectly conducting rough surface *J. Opt. Soc. Am.* **9** 1374–84
- [11] Maradudin A A, Nieto-Vesperinas M and Thorsos E 1994 Enhanced backscattering of light from randomly rough surfaces and related phenomena I: one-dimensional surfaces and angular correlation function of scattered field *Comments Condens. Matter Phys.* **17** 13–37
- [12] Nieto-Vesperinas M and Sanchez-Gil J A 1993 Intensity angular correlations of light multiply scattered from random rough surfaces *J. Opt. Soc. Am. A* **10** 150–7
- [13] Ishimaru A, Ailes-Sengers L, Phu P, Winebrenner D and Kuga Y 1994 Frequency and angular correlations of waves scattered by rough surfaces *Progress in Electromagnetics Research* vol 14 (Cambridge, MA: Elsevier Science) pp 1–34
- [14] Kuga Y, Lee C, Ishimaru A and Ailes-Sengers L 1997 Analytical, experimental, and numerical studies of angular memory signatures of waves scattered from one-dimensional rough surfaces *IEEE Trans. Geosci. Remote Sensing* **34** 1300–7
- [15] Chan T-K, Kuga Y and Ishimaru A 1995 Subsurface detection of buried object using angular correlation measurement *Waves Random Media* **7** 457–65
- [16] Tsang L, Zhang G and Pak K 1996 Detection of a buried object under a single random rough surface with angular correlation function in EM wave scattering *Microwave Opt. Technol. Lett.* **11** 300–4
- [17] Zhang G, Tsang L and Kuga Y 1997 Studies of the angular correlation function of scattering by random rough surfaces with and without a buried object *IEEE Trans. Geosci. Remote Sensing* **35** 444–53
- [18] Goff J A 1993 A unilitarian approach to modeling non-Gaussian characteristics of a topographic field *J. Geophys. Res.* **98** (B11) 19635–47
- [19] Tatarskii V I 1995 Characteristic functional for one class of non-Gaussian random functions *Waves Random Media* **5** 243–52
- [20] Tatarskii V I and Tatarskii V I 1996 Non-Gaussian statistical model of the ocean surface for wave-scattering theories *Waves Random Media* **6** 419–35
- [21] Johnson G E 1994 Constructions of particular random process *Proc. IEEE* **82** 270–84
- [22] Szajnowski W J 1977 The generation of correlated Weibull clutter for signal detection problem *IEEE Trans. Aerospace Electron. Syst.* **13** 536–40